Site-Resolved Exploration of High-Entropy Alloy Hydrogen Evolution Reaction Catalysts via Interpretable Modeling and High-Throughput Density Functional Theory

Hui Yang[a*], Delin Yuan[a], Hui Wei[a*], Zhe Zhou[a], Zhou-jun Wang[b], Chaonan Cui[b*]

[a]National Institute of Clean and Low Carbon Energy, Beijing 102211, PR China

[b]State Key Laboratory of Chemical Resource Engineering, Beijing Key Laboratory of Energy Environmental Catalysis, Beijing University of Chemical Technology, Beijing 100029, PR China

Corresponding Authors: 20112242@chnenergy.com.cn, hui.wei.d@chnenergy.com.cn, cuichn@buct.edu.cn

Computational Methods and Details

DFT calculations

All spin-polarized density functional theory (DFT) calculations were performed using the Vienna Ab initio Simulation Package (VASP),[1, 2] with workflows constructed and managed through the Atomic Simulation Environment (ASE).[3] The PAW (projector augmented-wave) potential[4] was employed to describe the interactions between ionic cores and valence electrons, and the exchange–correlation energy was treated within the generalized gradient approximation using the Perdew–Burke–Ernzerhof (GGA-PBE) functional.[5-7] A plane-wave energy cutoff of 400 eV was adopted for all calculations. To ensure sufficient surface site diversity while maintaining computational efficiency, all constructed HEA surfaces were expanded to (4 × 4) supercells with four atomic layers, in which the bottom two layers were fixed to simulate bulk constraints. A vacuum region of 20 Å was applied to all slabs along the surface normal direction to avoid interactions between periodic images. The Brillouin zone was sampled using the Monkhorst–Pack scheme with a 2 × 2 × 1 *k*-point mesh.[8] The Gaussian smearing with a width of 0.2 eV was employed for metallic systems. Structural optimizations were considered converged when the energy and maximum force on each atom converged to within 1×10^{-4} eV/atom and 0.05 eV/Å, respectively. Regarding van der Waals (vdW) interactions, while dispersion forces may make non-negligible contributions to adsorption energetics in heterogeneous systems,[9] the present work focuses on hydrogen chemisorption on metallic HEA surfaces, where the energetics are dominated by local metal–hydrogen bonding. Thus, explicit vdW corrections were omitted to maintain computational consistency across the large compositional space. Representative test calculations with vdW corrections (Table S5) show that although moderate quantitative shifts in ΔG_H occur, the overall adsorption trends and relative energetic preferences remain largely unchanged.

The computational hydrogen electrode (CHE) model was employed to evaluate the adsorption free energy of adsorbed hydrogen.[10] Within the CHE framework, the chemical potential of a proton–electron pair is equated to half of that of a hydrogen molecule in the gas phase under standard conditions, (i.e., $\mu(H^+ + e^-) = 1/2\ \mu(H_2(g))$). The effect of electrode potential was incorporated by shifting the electron energy by $-eU$, where e is the elementary charge and U is the applied electrode potential referenced to RHE. Accordingly, the ΔG_H was calculated as:

$$\Delta G_H = \Delta E_{ads} + \Delta E_{ZPE} - T\Delta S \quad \text{(Eq. 1)}$$

where ΔE_{ads} is the hydrogen adsorption energy obtained from DFT calculations, ΔE_{ZPE} is the zero-point energy correction, ΔS is the entropy change, and T is the temperature (298.15 K). All thermodynamic corrections were calculated using the VASPKIT package.[11]

Machine learning details for DSTAR and SISSO

To elucidate the relationship between the local coordination environment of active sites and their corresponding adsorption energies, the atomic configurations of sites must be transformed into machine-readable descriptors. Herein, the local atomic environments were characterized using the DSTAR descriptor, originally proposed by Seoin *et al.*, which has been successfully applied to bimetallic catalytic systems.[12] The DSTAR method describes each adsorption site by partitioning the local coordination environment into three regions: the first nearest neighbors (FNN), corresponding to the three metal atoms directly bonded to hydrogen; the same-layer of second nearest neighbors (SNN_{same}), which influence lateral electronic interactions on the surface; and the sublayer of second nearest neighbors (SNN_{sub}), which reflect subsurface-induced electronic and strain-related effects. For each region, the number of constituent metal atoms and the weighted elemental properties were calculated. Specifically, eleven tabulated atomic properties were employed, including atomic number. Ionic radius, oxidation state, electronegativity, row and group in periodic table, thermal conductivity, melting point, boiling point, block and ionization energy, resulting in a total of twelve features for each coordination region. Consequently, each adsorption site was represented by a 36-dimensional fingerprint (3 regions × 12 features), which quantitatively encodes the compositional, geometric and electronic characteristics of the local atomic environment (Fig. 1c and Fig. S5). These site-specific fingerprints were subsequently used as the primary input features for SISSO model training. Notably, the present descriptor set does not include explicit electronic-structure features such as the d-band center.[13, 14] While such descriptors can provide a deeper and more direct link between surface electronic structure and hydrogen adsorption strength, they generally require additional electronic-structure calculations for each adsorption configuration. Instead, the model relies on readily accessible elemental and physicochemical properties that implicitly capture the dominant chemical trends across diverse local environments. This choice avoids the additional computational cost of per-site electronic-structure post-processing, enabling efficient exploration of the broad FCC-HEA compositional space. This strategy positions the present framework as complementary to electronic-descriptor approaches, with future incorporation of electronic-structure descriptors offering a clear path to further enhancing both predictive accuracy and mechanistic insight.

The resulting SISSO models enable efficient prediction of ΔG_H for all surface sites across the FCC-HEA composition space. Specifically, the SISSO model was trained and validated using a reproducible data partitioning strategy through the train_test_split function in scikit-learn. The full dataset comprising 7004 adsorption sites was randomly split into a training set (80%, 5603 sites) and a testing set (20%, 1401 sites) with a fixed random seed of 42. All hyperparameter tuning and model selection were conducted exclusively on the training set, and the testing set was strictly held out for final, unbiased performance evaluation.

Machine learning details for phase prediction

A supervised machine-learning classifier was employed to pre-screen FCC-stable Ni-based high-entropy alloy compositions prior to DFT evaluation, reducing the computational burden of exhaustive phase identification. The model was trained on a literature-derived curated dataset consisting of 369 experimentally reported multicomponent alloys with reliable crystal phase labels (FCC, BCC, and others).

Ten physically interpretable descriptors were adopted as input features, covering elemental, alloy-level, and thermodynamic characteristics, including composition-weighted averages of atomic radius ($\bar{r}$), valence electron concentration ($\overline{VEC}$), Pauling electronegativity ($\bar{\chi}$), and melting point ($\overline{T_m}$); atomic size mismatch (δ), electronegativity difference (Δχ), mixing entropy (ΔS_{mix}), mixing enthalpy (ΔH_{mix}); and thermodynamic criteria Ω and Λ. All descriptor definitions and calculation formulas are provided as following:

$$\bar{r} = \sum_i c_i r_i$$

$$\overline{VEC} = \sum_i c_i \, VEC_i$$

$$\bar{\chi} = \sum_i c_i \chi_i$$

$$\overline{T_m} = \sum_i c_i T_m^i$$

$$\delta = \sqrt{\sum_{i=1}^{n} c_i (1 - r_i / \sum_{j=1}^{n} c_j r_j)^2}$$

$$\Delta\chi = \sqrt{\sum_{i=1}^{n} c_i (\chi_i - \sum_{j=1}^{n} c_j \chi_j)^2}$$

$$\Delta S_{mix} = -R \sum_{i=1}^{n} c_i \ln c_i$$

$$\Delta H_{mix} = \sum_{i=1, j>i}^{n} 4 \Delta H_{ij}^{mix} c_i c_j$$

$$\Omega = \frac{T_m \Delta S_{mix}}{|\Delta H_{mix}|}$$

$$\Lambda = \frac{\Delta S_{mix}}{\delta^2}$$

where the individual items involved are defined as follows. The c_i (and c_j), r_i (and r_j), χ_i (and χ_j), VEC_i and T_m^i are the atomic molar fraction, atomic radius, Pauling electronegativity, valence electron number, and melting point of the i^{th} (and j^{th}) element, respectively. R is the gas constant. ΔH_{ij}^{mix} is the enthalpy of mixing for the binary equimolar *i-j* alloys.

Six widely used classification algorithms—Logistic Regression, Support Vector Machine (SVM), Gaussian Process Classifier (GPC), Random Forest (RF), XGBoost, and Multi-Layer Perceptron (MLP)—were benchmarked using 10-fold cross-validation. The MLP model achieved the highest average accuracy of 0.89 and was therefore selected as the final phase classifier. It should be noted that this ML phase filter serves as a pre-screening step to efficiently exclude non-FCC compositions before high-throughput DFT calculations, rather than a definitive phase predictor.

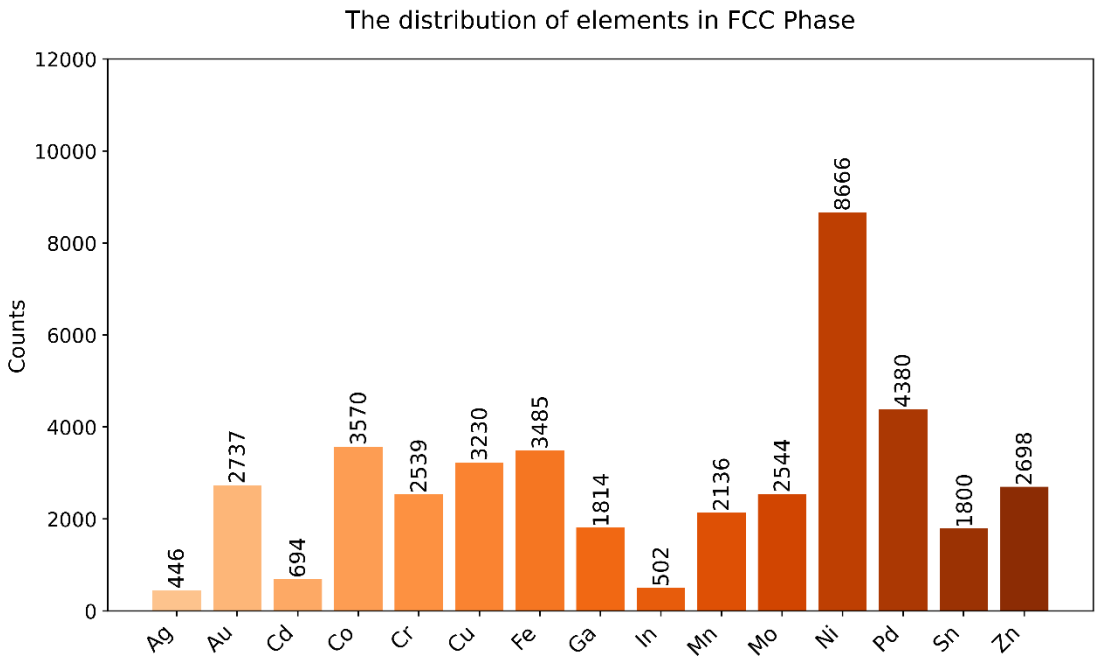

Figure S1. Bar chart illustrating the distribution of elements in the Face-Centered Cubic (FCC) phase. The x-axis displays 15 elements (Ag, Au, Cd, Co, Cr, Cu, Fe, Ga, In, Mn, Mo, Ni, Pd, Sn, Zn), while the y-axis quantifies their abundance (Counts).

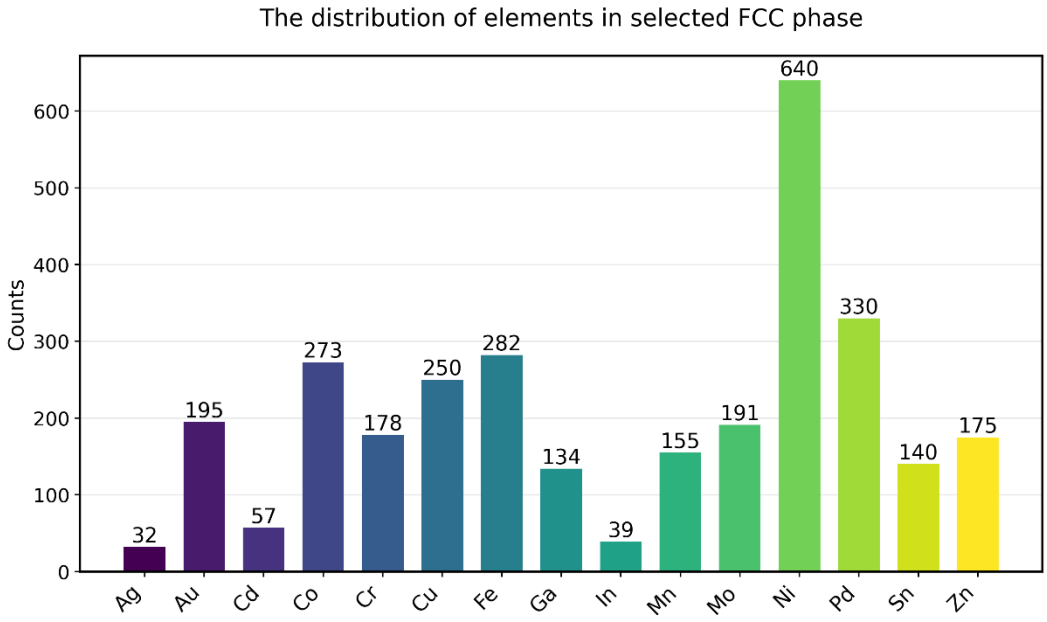

Figure S2. Bar chart illustrating the distribution of elements in selected Face-Centered Cubic (FCC) phase. The x-axis displays 15 elements (Ag, Au, Cd, Co, Cr, Cu, Fe, Ga, In, Mn, Mo, Ni, Pd, Sn, Zn), while the y-axis quantifies their abundance (Counts).

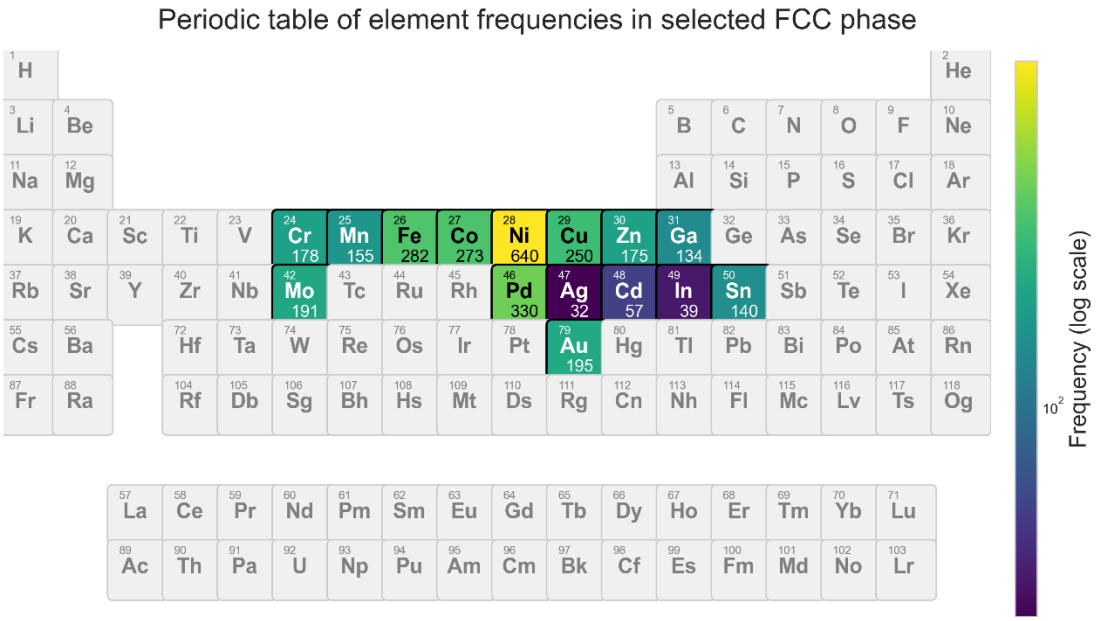

Figure S3. Elemental frequency distribution of screened FCC high-entropy alloys, visualized on the periodic table to illustrate the relative occurrence of elements across the selected compositions.

S1.
$Co_1Cr_1Cd_1In_1Ni_{16}$

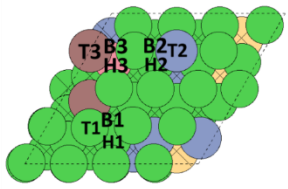

Sites	ΔG_H (eV)
T1	-0.53 (H)
B1	-0.43 (H1)
H1	-0.41
T2	-0.54 (H)
B2	-0.48 (H)
H2	-0.41
T3	-0.40 (H)
B3	-0.45 (H)
H3	-0.44

S2.
$Co_1Cr_1Ga_5Au_1Ni_{12}$

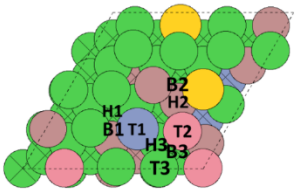

Sites	ΔG_H (eV)
T1	-0.47 (H3)
B1	-0.58 (H)
H1	-0.54
T2	-0.48 (H)
B2	-0.24 (B)
H2	0.14
T3	-0.41 (H)
B3	-0.48 (H3)
H3	-0.48

S3.
$Cu_{13}Fe_1Co_1Pd_1Ni_4$

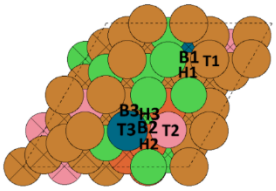

Sites	ΔG_H (eV)
T1	-0.22 (H)
B1	-0.30 (H1)
H1	-0.30
T2	-0.32 (H3)
B2	-0.30 (H2)
H2	-0.29
T3	-0.32 (H3)
B3	-0.31 (H3)
H3	-0.31

Figure S4. Corresponding hydrogen adsorption free energies (ΔG_H) for local atomic configurations on selected HEA surfaces. Green, dark yellow, yellow, dark blue, purple, brown, white yellow, orange, dark pink and pink balls represent Ni, Cu, Au, Pd, Cr, In, Cd, Fe, Ga, and Co atoms, respectively. Various types of adsorption sites are labeled as T (top), B (bridge), and H (hollow), and the numbers in parentheses (e.g., H3) correspond to the specific sites indicated in the surface structures above.

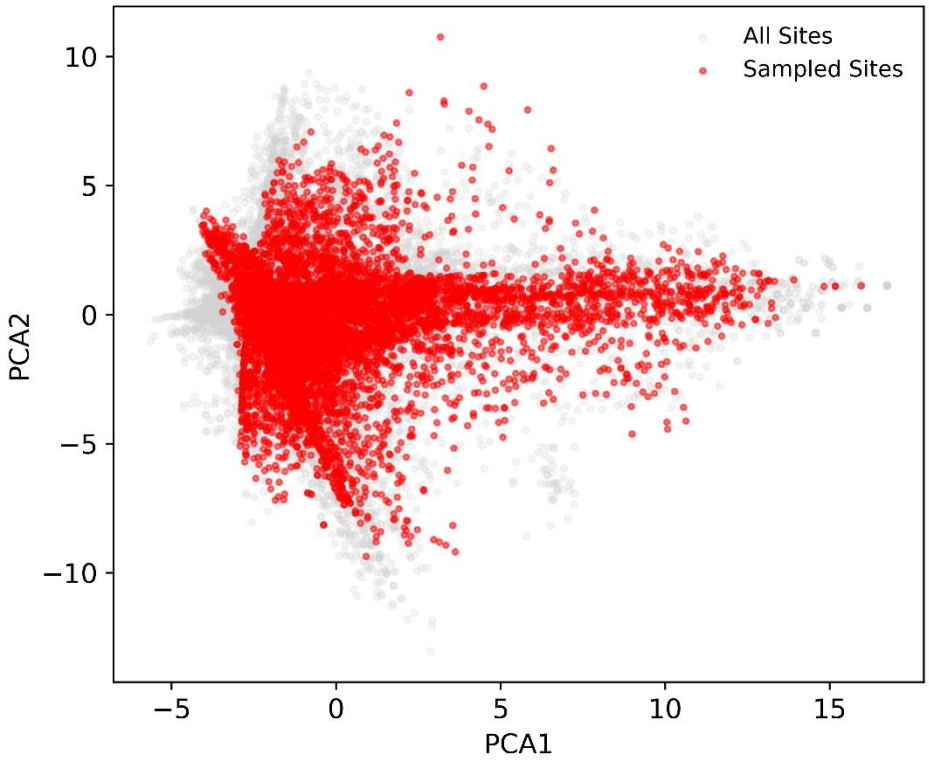

Figure S5. PCA projection of the full candidate-site pool (gray) and the sampled adsorption configurations used for DFT calculations (red). The sampled configurations show broad overlap with the dominant descriptor distribution, indicating representative coverage of the relevant local-environment space.

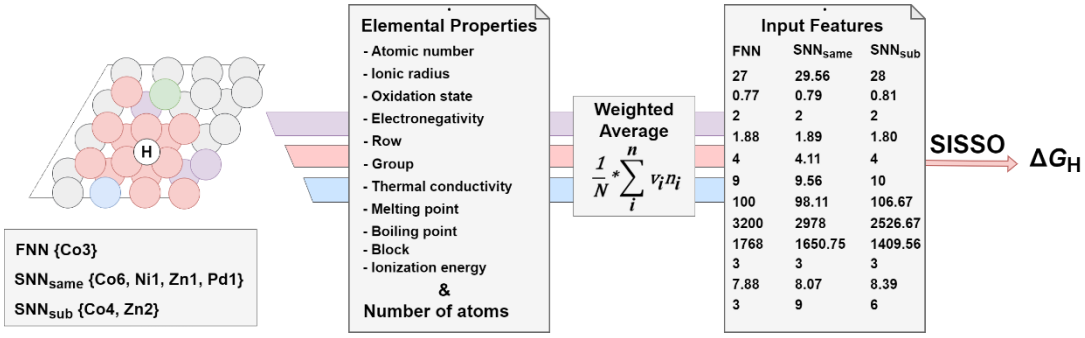

Figure. S6 An example of fingerprint construction for H adsorption on HEA surface, in which the pink, purple, green, blue balls represent the Co, Zn, Ni and Pd, respectively.

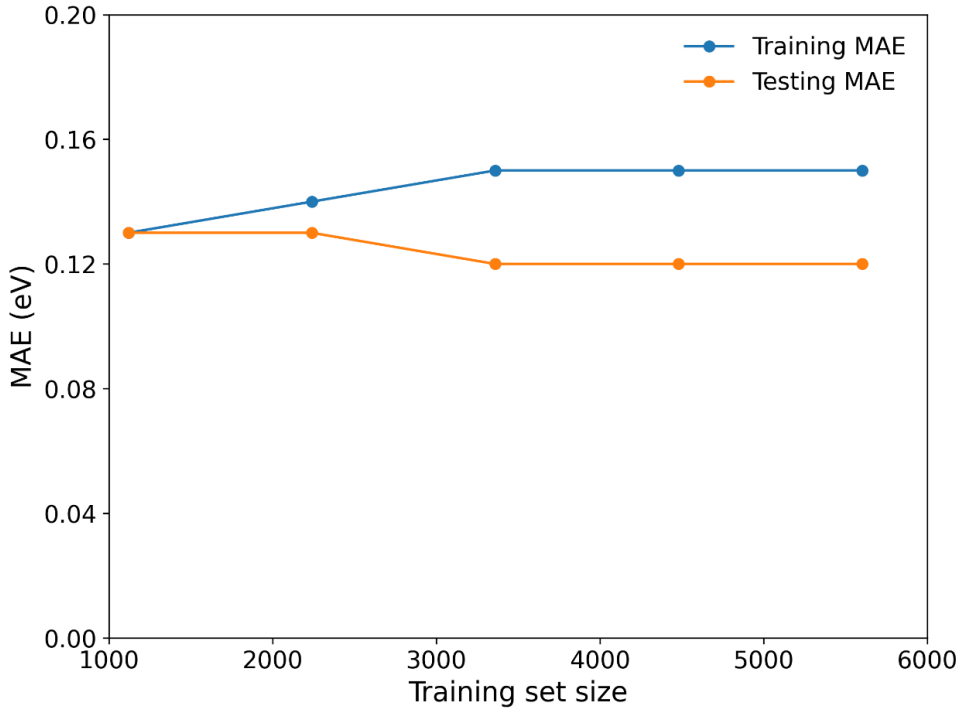

Figure. S7 Learning curves of the SISSO model. The plot shows the evolution of the mean absolute error (MAE) for both the training (blue) and testing (orange) sets as a function of the training set size. The model achieves convergence with a test MAE stabilizing at approximately 0.12 eV beyond 3,500 training samples, indicating robust generalization without overfitting.

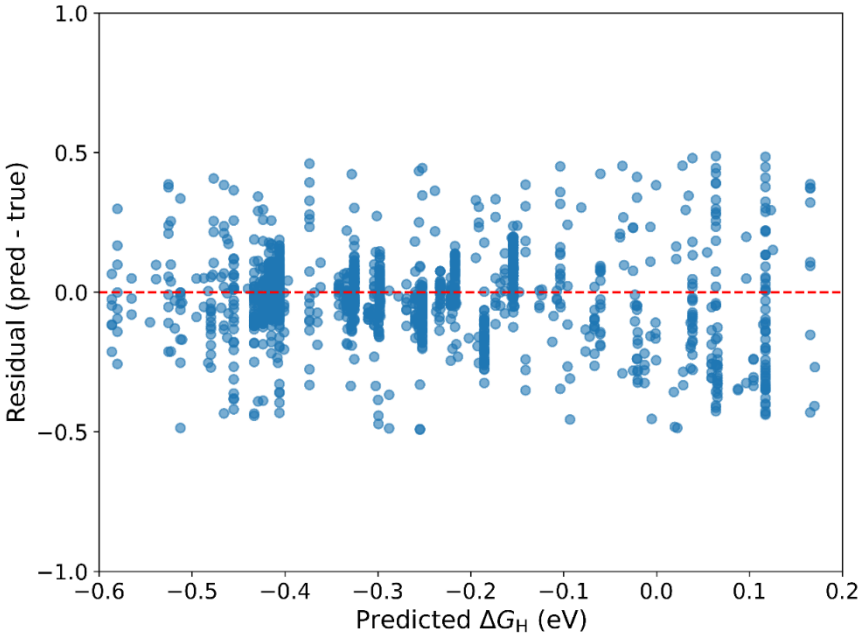

Figure. S8 Residual analysis of the model predictions. The residuals are randomly scattered around the zero line (dashed red) with no discernible trend, confirming the absence of systematic bias in the model.

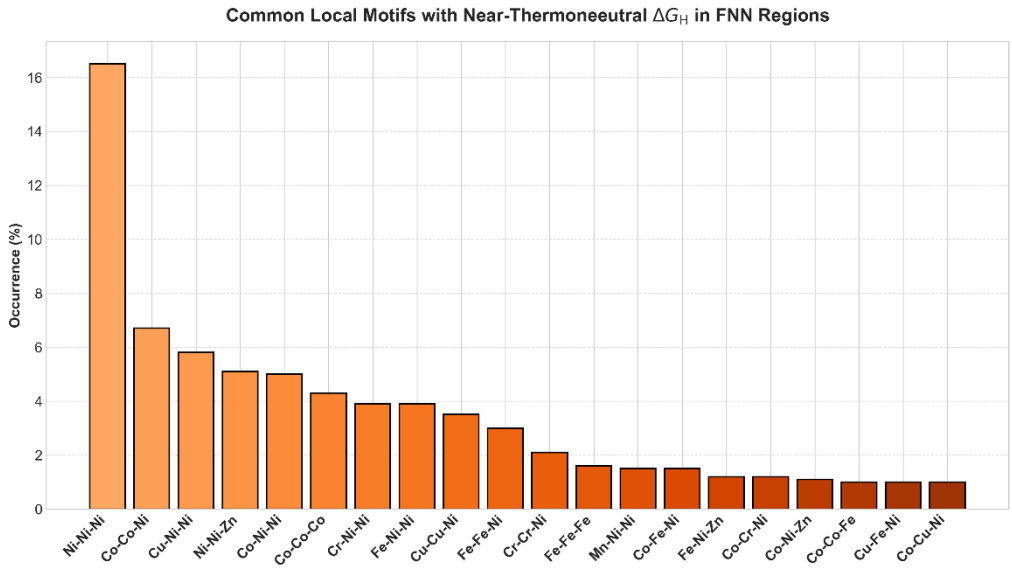

Figure S9. Statistical distribution of the most frequent local elemental motifs in FNN regions associated with near-thermoneutral hydrogen adsorption site.

Table S1. Molar ratios of the HEA compositions in the selected FCC phases.

$Ag_1Au_1Cu_1Pd_{13}Ni_4$	$Ag_1Cu_9Mo_1Pd_5Ni_4$	$Au_1Co_{13}Mn_1Pd_1Ni_4$	$Au_1Co_5Mn_1Sn_1Ni_{12}$	$Au_1Cu_1Fe_5Mn_1Ni_{12}$
$Ag_1Au_5Fe_1Pd_9Ni_4$	$Ag_1Fe_1Ga_1Pd_9Ni_8$	$Au_1Co_1Cr_1Ga_5Ni_{12}$	$Au_1Co_5Pd_5Sn_1Ni_8$	$Au_1Cu_1Fe_5Zn_5Ni_8$
$Ag_1Au_9Fe_1Pd_5Ni_4$	$Ag_1Fe_1Mo_1Pd_{13}Ni_4$	$Au_1Co_1Cr_1Mn_1Ni_{16}$	$Au_1Co_9Cr_1Mo_5Ni_4$	$Au_1Cu_1In_1Pd_{13}Ni_4$
$Ag_1Au_9Mo_1Pd_5Ni_4$	$Ag_1Fe_5Mn_1Mo_5Ni_8$	$Au_1Co_1Cu_1Mo_5Ni_{12}$	$Au_1Co_9Cr_5Cu_1Ni_4$	$Au_1Cu_1Mo_5Pd_1Ni_{12}$
$Ag_1Cd_1Co_1Pd_9Ni_8$	$Ag_1Fe_5Mo_1Pd_9Ni_4$	$Au_1Co_1Cu_9Ga_5Ni_4$	$Au_1Co_9Cr_5Ga_1Ni_4$	$Au_1Cu_1Pd_1Zn_1Ni_{16}$
$Ag_1Cd_1Cr_1Pd_9Ni_8$	$Ag_1Fe_9Mn_1Pd_5Ni_4$	$Au_1Co_1Fe_1Pd_1Ni_{16}$	$Au_1Co_9Cu_1Fe_5Ni_4$	$Au_1Cu_1Pd_9Sn_1Ni_8$
$Ag_1Cd_1Cu_1Pd_9Ni_8$	$Ag_1Fe_9Pd_5Zn_1Ni_4$	$Au_1Co_1Fe_1Zn_{13}Ni_4$	$Au_1Co_9Ga_1Mo_1Ni_8$	$Au_1Cu_5Fe_1Mo_9Ni_4$
$Ag_1Co_1Pd_{13}Sn_1Ni_4$	$Ag_1In_1Mo_1Pd_{13}Ni_4$	$Au_1Co_1Fe_5Ga_1Ni_{12}$	$Au_1Cr_1Cu_1Ga_1Ni_{16}$	$Au_1Cu_5Fe_5Ga_1Ni_8$
$Ag_1Co_1Pd_{13}Zn_1Ni_4$	$Au_{13}Co_1Cr_1Cu_1Ni_4$	$Au_1Co_1Fe_9Pd_5Ni_4$	$Au_1Cr_1Fe_1Mo_1Ni_{16}$	$Au_1Cu_5Fe_5Mo_5Ni_4$
$Ag_1Co_5Cu_1Pd_9Ni_4$	$Au_{13}Cr_1Cu_1Mo_1Ni_4$	$Au_1Co_1In_1Pd_9Ni_8$	$Au_1Cr_1Fe_5Mn_1Ni_{12}$	$Au_1Cu_5Fe_5Pd_1Ni_8$
$Ag_1Co_5Cu_5Mo_5Ni_4$	$Au_{13}Cr_1Fe_1Mo_1Ni_4$	$Au_1Co_1Mn_5Zn_9Ni_4$	$Au_1Cr_1Fe_5Pd_5Ni_8$	$Au_1Cu_5Mn_1Mo_1Ni_{12}$
$Ag_1Co_5Fe_5Mn_5Ni_4$	$Au_{13}Cu_1Fe_1Zn_1Ni_4$	$Au_1Co_5Cr_1Mn_1Ni_{12}$	$Au_1Cr_1Ga_1Zn_9Ni_8$	$Au_1Cu_5Mo_1Pd_9Ni_4$
$Ag_1Co_5In_1Pd_9Ni_4$	$Au_{13}Cu_1Ga_1Pd_1Ni_4$	$Au_1Co_5Cr_1Sn_1Ni_{12}$	$Au_1Cr_1Pd_5Zn_5Ni_8$	$Au_1Cu_9Fe_1Mn_5Ni_4$
$Ag_1Co_5Pd_5Sn_5Ni_4$	$Au_{13}Fe_1Ga_1Zn_1Ni_4$	$Au_1Co_5Cr_5Pd_5Ni_4$	$Au_1Cr_1Sn_1Zn_9Ni_8$	$Au_1Cu_9Fe_1Mo_5Ni_4$
$Ag_1Co_9Cr_1Ga_1Ni_8$	$Au_{13}Ga_1Mn_1Pd_1Ni_4$	$Au_1Co_5Cu_5Ga_5Ni_4$	$Au_1Cr_5Cu_5Fe_1Ni_8$	$Au_1Cu_9Mn_5Pd_1Ni_4$
$Ag_1Cu_1Fe_1Pd_5Ni_{12}$	$Au_1Cd_1Ga_1Pd_{13}Ni_4$	$Au_1Co_5Cu_9Sn_1Ni_4$	$Au_1Cr_5Cu_5Pd_1Ni_8$	$Au_1Cu_9Pd_1Sn_1Ni_8$
$Ag_1Cu_5Mn_1Pd_9Ni_4$	$Au_1Cd_1In_1Pd_{13}Ni_4$	$Au_1Co_5Ga_1Mo_5Ni_8$	$Au_1Cr_5Cu_5Sn_1Ni_8$	$Au_1Fe_1Ga_1Pd_{13}Ni_4$
$Ag_1Cu_5Mo_1Pd_5Ni_8$	$Au_1Cd_1Pd_5Zn_1Ni_{12}$	$Au_1Co_5Ga_5Pd_1Ni_8$	$Au_1Cr_5Fe_1Pd_1Ni_{12}$	$Au_1Fe_1Ga_1Zn_9Ni_8$
$Ag_1Cu_5Pd_5Sn_5Ni_4$	$Au_1Cd_5Fe_1Sn_5Ni_8$	$Au_1Co_5In_1Pd_9Ni_4$	$Au_1Cr_5Fe_5Mo_1Ni_8$	$Au_1Fe_1In_1Pd_9Ni_8$
$Ag_1Cu_5Pd_5Zn_1Ni_8$	$Au_1Co_{13}Cu_1Sn_1Ni_4$	$Au_1Co_5Mn_1Mo_1Ni_{12}$	$Au_1Cu_1Fe_1Mn_5Ni_{12}$	$Au_1Fe_1Mo_1Zn_5Ni_{12}$
$Ag_1Cu_5Pd_9Zn_1Ni_4$	$Au_1Co_{13}Fe_1Mn_1Ni_4$	$Au_1Co_5Mn_1Pd_1Ni_{12}$	$Au_1Cu_1Fe_1Zn_{13}Ni_4$	$Au_1Fe_1Pd_5Sn_1Ni_{12}$
$Au_1Fe_1Pd_5Zn_5Ni_8$	$Au_1Co_{13}Ga_1Mn_1Ni_4$	$Au_1Ga_1Sn_1Zn_5Ni_{12}$	$Au_5Co_1Cu_1Pd_5Ni_8$	$Au_5Co_1Fe_5Zn_5Ni_4$
$Au_1Fe_5Mn_1Mo_1Ni_{12}$	$Au_1Fe_5Pd_5Sn_1Ni_8$	$Au_1In_1Pd_5Zn_1Ni_{12}$	$Au_5Co_1Cu_5Mn_5Ni_4$	$Au_5Co_1In_1Pd_5Ni_8$
$Au_1Fe_5Mn_5Zn_5Ni_4$	$Au_1Fe_5Pd_9Zn_1Ni_4$	$Au_1Mo_1Pd_{13}Sn_1Ni_4$	$Au_5Co_1Cu_5Pd_5Ni_4$	$Au_5Co_1Mn_1Pd_1Ni_{12}$
$Au_1Fe_5Mo_1Pd_5Ni_8$	$Au_1Fe_9Mn_1Pd_1Ni_8$	$Au_1Pd_5Sn_5Zn_1Ni_8$	$Au_5Co_1Fe_1Mn_1Ni_{12}$	$Au_5Co_1Mo_5Zn_1Ni_8$
$Au_1Fe_5Mo_5Pd_5Ni_4$	$Au_1Fe_9Pd_1Zn_5Ni_4$	$Au_5Co_1Cr_5Pd_1Ni_8$	$Au_5Co_1Fe_1Pd_5Ni_8$	$Au_5Co_5Cr_5Pd_1Ni_4$
$Ag_1Fe_5Mo_5Ni_9$	$Au_1Ga_1Mo_5Pd_9Ni_4$	$Au_1Fe_1Zn_5Ni_{13}$	$Au_5Cu_9Fe_5Ni_1$	$Au_9Cu_9Fe_1Ni_1$
$Ag_1Mo_1Pd_{17}Ni_1$	$Au_{17}Ga_1Sn_1Ni_1$	$Au_1Fe_5Mn_5Ni_9$	$Au_5Cu_9Pd_5Ni_1$	$Au_9Cu_9Sn_1Ni_1$
$Ag_9Cd_9Pd_1Ni_1$	$Au_{17}Mo_1Zn_1Ni_1$	$Au_1Fe_9Mn_1Ni_9$	$Au_5Fe_1Zn_1Ni_{13}$	$Au_9Ga_1Pd_1Ni_9$
$Au_{13}Cu_5Mn_1Ni_1$	$Au_1Co_1Pd_1Ni_{17}$	$Au_1Fe_9Zn_5Ni_5$	$Au_5Fe_5Ga_1Ni_9$	$Au_9Mo_1Zn_1Ni_9$
$Au_{13}Fe_1Pd_5Ni_1$	$Au_1Co_9Fe_5Ni_5$	$Au_1Ga_1Pd_{13}Ni_5$	$Au_5Fe_5Pd_9Ni_1$	$Cd_1Co_5Pd_{13}Ni_1$
$Au_{13}Pd_5Sn_1Ni_1$	$Au_1Cr_1Cu_1Ni_{17}$	$Au_1Ga_1Pd_5Ni_{13}$	$Au_5Mo_1Zn_1Ni_{13}$	$Cd_1Cr_1Pd_9Ni_9$
$Au_{17}Co_1Cr_1Ni_1$	$Au_1Cr_1Fe_5Ni_{13}$	$Au_1Mn_1Zn_9Ni_9$	$Au_9Co_1Fe_1Ni_9$	$Cd_1Fe_1Pd_5Ni_{13}$
$Au_{17}Cr_1Mo_1Ni_1$	$Au_1Cr_1Zn_5Ni_{13}$	$Au_5Co_1Fe_9Ni_5$	$Au_9Co_1Pd_1Ni_9$	$Co_{13}Fe_1Mo_1Ni_5$
$Au_{17}Fe_1Sn_1Ni_1$	$Au_1Cr_1Zn_9Ni_9$	$Au_5Cr_1Pd_{13}Ni_1$	$Au_9Cr_5Pd_5Ni_1$	$Co_{13}Pd_1Zn_5Ni_1$
$Au_{17}Ga_1Mn_1Ni_1$	$Au_1Cr_5Cu_5Ni_9$	$Au_5Cu_1Fe_1Ni_{13}$	$Au_9Cu_5Fe_5Ni_1$	$Co_{17}Cr_1Zn_1Ni_1$
$Au_5Co_5Fe_5Pd_1Ni_4$	$Au_1Cu_{17}Fe_1Ni_1$	$Co_1Cu_9Mo_1Ni_9$	$Co_5Cu_5In_1Ni_9$	$Au_5Cu_1Fe_9Mn_1Ni_4$
$Au_5Co_5Mo_1Zn_1Ni_8$	$Co_{17}Fe_1Mo_1Ni_1$	$Co_1Fe_1Sn_1Ni_{17}$	$Co_5Cu_9Ga_5Ni_1$	$Au_5Cu_1Ga_1Pd_1Ni_{12}$
$Au_5Co_9Cr_1Pd_1Ni_4$	$Co_{17}Fe_1Zn_1Ni_1$	$Co_1Fe_5Ga_1Ni_{13}$	$Co_5Fe_{13}Ga_1Ni_1$	$Au_5Cu_1Mo_1Zn_5Ni_8$
$Au_5Co_9Cr_1Sn_1Ni_4$	$Co_{17}Ga_1Pd_1Ni_1$	$Co_1Fe_9Mn_5Ni_5$	$Co_5Fe_{13}Mo_1Ni_1$	$Au_5Cu_1Mo_9Sn_1Ni_4$
$Au_5Co_9Fe_1Pd_1Ni_4$	$Co_1Cr_1Ga_1Ni_{17}$	$Co_1Fe_9Mo_1Ni_9$	$Co_5Ga_5Pd_1Ni_9$	$Au_5Cu_1Pd_5Sn_1Ni_8$
$Au_5Co_9Mn_1Sn_1Ni_4$	$Co_1Cr_1Zn_5Ni_{13}$	$Co_1Fe_9Pd_5Ni_5$	$Co_5Mo_1Pd_5Ni_9$	$Au_5Cu_1Pd_5Zn_5Ni_4$
$Au_5Cr_1Cu_1Mo_5Ni_8$	$Co_1Cr_5Cu_9Ni_5$	$Co_1Ga_1Pd_9Ni_9$	$Co_5Pd_{13}Zn_1Ni_1$	$Au_5Cu_5Fe_1Sn_1Ni_8$

$Au_5Cr_1Fe_5Mo_5Ni_4$	$Co_1Cr_5Fe_5Ni_9$	$Co_1Mn_1Pd_5Ni_{13}$	$Co_9Fe_1Mo_1Ni_9$	$Au_5Cu_5Pd_5Sn_1Ni_4$
$Au_5Cr_1Mo_1Pd_1Ni_{12}$	$Co_1Cu_{13}Mo_1Ni_5$	$Co_1Mo_5Pd_9Ni_5$	$Co_9Fe_5Mo_1Ni_5$	$Au_5Cu_5Sn_1Zn_5Ni_4$
$Au_5Cu_1Fe_5Mo_5Ni_4$	$Co_1Cu_{13}Pd_5Ni_1$	$Co_5Cr_5Pd_9Ni_1$	$Co_9Fe_5Sn_1Ni_5$	$Au_5Fe_1Mo_5Pd_1Ni_8$
$Au_5Fe_5Mn_1Sn_1Ni_8$	$Co_1Cu_1Fe_{13}Ni_5$	$Cr_1Mo_1Zn_1Ni_{17}$	$Cu_1Fe_5Ga_5Ni_9$	$Au_9Co_5Mo_1Sn_1Ni_4$
$Au_5Ga_1Mo_1Sn_1Ni_{12}$	$Co_9Fe_9Ga_1Ni_1$	$Cr_5Cu_1Fe_9Ni_5$	$Cu_1Fe_5Zn_5Ni_9$	$Au_9Cr_1Cu_1Sn_1Ni_8$
$Au_5Pd_5Sn_5Zn_1Ni_4$	$Co_9Mo_1Zn_9Ni_1$	$Cr_5Cu_9Zn_1Ni_5$	$Cu_1Fe_9Mn_5Ni_5$	$Au_9Cr_1Cu_5Mo_1Ni_4$
$Au_9Cd_1Cr_1Pd_5Ni_4$	$Co_9Mo_5Pd_5Ni_1$	$Cr_5Fe_5Ga_1Ni_9$	$Cu_1Fe_9Pd_1Ni_9$	$Au_9Cr_1Fe_1Zn_1Ni_8$
$Au_9Cd_1Pd_5Zn_1Ni_4$	$Cr_1Cu_1Fe_9Ni_9$	$Cr_5Fe_5Mn_1Ni_9$	$Cu_1Ga_1Pd_{13}Ni_5$	$Au_9Cr_1Ga_1Mo_1Ni_8$
$Au_9Co_1Cr_1Pd_5Ni_4$	$Cr_1Cu_5Mn_1Ni_{13}$	$Cr_5Mo_1Pd_5Ni_9$	$Cu_1Ga_1Zn_{13}Ni_5$	$Au_9Cr_1Ga_1Pd_1Ni_8$
$Au_9Co_1Cu_5Mo_1Ni_4$	$Cr_1Fe_1Ga_1Ni_{17}$	$Cu_{13}Fe_1Mn_1Ni_5$	$Cu_1Mn_1Pd_{13}Ni_5$	$Au_9Cu_1Fe_1Ga_1Ni_8$
$Au_9Co_1Ga_1Pd_5Ni_4$	$Cr_1Fe_1Sn_1Ni_{17}$	$Cu_{13}Mo_1Pd_1Ni_5$	$Cu_1Mn_5Pd_1Ni_{13}$	$Au_9Cu_1Ga_1Pd_1Ni_8$
$Au_9Co_1In_1Pd_5Ni_4$	$Cr_1Fe_5Mn_1Ni_{13}$	$Cu_1Fe_1Ga_5Ni_{13}$	$Cu_1Mo_5Zn_1Ni_{13}$	$Au_9Cu_1Mn_1Sn_1Ni_8$
$Au_9Co_5Cr_1Mn_1Ni_4$	$Cr_1Mn_1Zn_1Ni_{17}$	$Cu_1Fe_1Pd_9Ni_9$	$Cu_1Pd_1Zn_1Ni_{17}$	$Au_9Cu_1Mo_1Zn_1Ni_8$
$Au_9Cu_1Mo_5Sn_1Ni_4$	$Cr_1Mn_5Pd_9Ni_5$	$Fe_1Mn_1Zn_5Ni_{13}$	$Cd_1Co_1Cu_1Fe_5Ni_{12}$	$Cd_1Co_5Mo_1Zn_1Ni_{12}$
$Au_9Cu_1Sn_1Zn_5Ni_4$	$Cu_1Pd_5Sn_5Ni_9$	$Fe_1Mo_5Pd_9Ni_5$	$Cd_1Co_1Mn_1Pd_9Ni_8$	$Cd_1Co_5Pd_1Zn_1Ni_{12}$
$Au_9Cu_5Mo_1Zn_1Ni_4$	$Cu_1Sn_1Zn_9Ni_9$	$Fe_1Pd_1Sn_1Ni_{17}$	$Cd_1Co_1Mo_1Pd_{13}Ni_4$	$Cd_1Co_5Pd_1Zn_5Ni_8$
$Au_9Cu_5Pd_1Zn_1Ni_4$	$Cu_5Mn_1Sn_1Ni_{13}$	$Fe_5Mn_5Pd_1Ni_9$	$Cd_1Co_1Pd_5Zn_5Ni_8$	$Cd_1Co_5Pd_9Sn_1Ni_4$
$Au_9Fe_1Ga_1Mo_1Ni_8$	$Cu_5Sn_1Zn_1Ni_{13}$	$Fe_5Mo_5Pd_1Ni_9$	$Cd_1Co_5Cu_1Fe_9Ni_4$	$Cd_1Co_5Pd_9Zn_1Ni_4$
$Au_9Fe_1Mo_1Zn_5Ni_4$	$Cu_9Fe_1Pd_1Ni_9$	$Fe_5Sn_1Zn_5Ni_9$	$Cd_1Co_5Cu_1Mo_1Ni_{12}$	$Cd_1Co_9Cr_5In_1Ni_4$
$Au_9Ga_1In_1Pd_5Ni_4$	$Cu_9Mn_1Pd_5Ni_5$	$Fe_9Ga_1Mo_1Ni_9$	$Cd_1Co_5Cu_9Fe_1Ni_4$	$Cd_1Co_9Cu_1Pd_5Ni_4$
$Au_9Mn_1Mo_5Sn_1Ni_4$	$Cu_9Mo_1Pd_1Ni_9$	$Fe_9Mn_1Zn_1Ni_9$	$Cd_1Co_5Fe_1Ga_1Ni_{12}$	$Cd_1Co_9Cu_5Ga_1Ni_4$
$Cd_1Co_1Cr_1In_1Ni_{16}$	$Fe_{13}Mn_1Pd_1Ni_5$	$Ga_1Mn_1Pd_1Ni_{17}$	$Cd_1Co_5Fe_9Sn_1Ni_4$	$Cd_1Co_9Fe_1Mo_1Ni_8$
$Cd_1Co_1Cr_5Fe_5Ni_8$	$Fe_{13}Sn_1Zn_1Ni_5$	$Cd_5Co_1Cr_1Pd_1Ni_{12}$	$Cd_1Co_5Mo_1Pd_5Ni_8$	$Cd_1Co_9Fe_5Pd_1Ni_4$
$Cd_1Co_9Ga_1Mo_1Ni_8$	$Fe_1Ga_1Zn_{13}Ni_5$	$Cd_5In_5Mn_5Zn_1Ni_4$	$Co_1Cr_1Fe_5Mn_5Ni_8$	$Co_1Cr_5Cu_1Mn_1Ni_{12}$
$Cd_1Co_9Mo_1Pd_5Ni_4$	$Cd_1Fe_1Mn_1Pd_{13}Ni_4$	$Co_{13}Cr_1Mn_1Mo_1Ni_4$	$Co_1Cr_1Fe_5Mo_1Ni_{12}$	$Co_1Cr_5Cu_1Pd_9Ni_4$
$Cd_1Cr_1In_1Pd_9Ni_8$	$Cd_1Fe_1Mn_1Pd_9Ni_8$	$Co_{13}Fe_1Mn_1Zn_1Ni_4$	$Co_1Cr_1Fe_5Sn_1Ni_{12}$	$Co_1Cr_5Cu_5Mo_1Ni_8$
$Cd_1Cr_5Fe_1Pd_5Ni_8$	$Cd_1Fe_1Pd_5Zn_5Ni_8$	$Co_{13}Ga_1Mo_1Pd_1Ni_4$	$Co_1Cr_1Fe_9Zn_1Ni_8$	$Co_1Cr_5Cu_5Zn_1Ni_8$
$Cd_1Cu_1Fe_5Pd_5Ni_8$	$Cd_1Fe_5Ga_1Pd_1Ni_{12}$	$Co_{13}Mn_1Mo_1Zn_1Ni_4$	$Co_1Cr_1Ga_1Mn_5Ni_{12}$	$Co_1Cr_5Ga_1Pd_1Ni_{12}$
$Cd_1Cu_1Fe_5Pd_9Ni_4$	$Cd_1Fe_5Pd_9Zn_1Ni_4$	$Co_1Cr_1Cu_5Mn_5Ni_8$	$Co_1Cr_1Mn_1Zn_9Ni_8$	$Co_1Cr_5Mn_1Zn_9Ni_4$
$Cd_1Cu_1Mn_1Pd_9Ni_8$	$Cd_1Fe_9In_1Pd_5Ni_4$	$Co_1Cr_1Cu_5Mo_1Ni_{12}$	$Co_1Cr_1Mo_5Pd_1Ni_{12}$	$Co_1Cr_5Pd_9Sn_1Ni_4$
$Cd_1Cu_1Pd_1Zn_5Ni_{12}$	$Cd_1Ga_1Mn_1Pd_9Ni_8$	$Co_1Cr_1Fe_5Ga_1Ni_{12}$	$Co_1Cr_1Pd_1Zn_9Ni_8$	$Co_1Cr_9Cu_5Pd_1Ni_4$
$Cd_1Cu_5Mo_5Pd_5Ni_4$	$Cd_1Mn_1Pd_{13}Zn_1Ni_4$	$Co_1Cr_1Fe_5Mn_1Ni_{12}$	$Co_1Cr_1Pd_5Sn_5Ni_8$	$Co_1Cu_{13}Fe_1Pd_1Ni_4$
$Cd_1Cu_5Pd_5Sn_5Ni_4$	$Cd_1Mo_5Pd_9Sn_1Ni_4$	$Co_1Fe_1Mn_5Pd_5Ni_8$	$Co_1Cr_1Sn_1Zn_9Ni_8$	$Co_1Cu_{13}Mo_1Zn_1Ni_4$
$Co_1Cu_1Fe_{13}Mo_1Ni_4$	$Cd_1Pd_5Sn_5Zn_1Ni_8$	$Co_1Fe_1Mn_5Pd_9Ni_4$	$Co_1Ga_1Sn_1Zn_5Ni_{12}$	$Co_5Cr_1Cu_5Sn_1Ni_8$
$Co_1Cu_1Fe_1Ga_1Ni_{16}$	$Co_1Cu_5Fe_5Pd_1Ni_8$	$Co_1Fe_1Mo_1Zn_9Ni_8$	$Co_1In_1Mn_1Pd_{13}Ni_4$	$Co_5Cr_1Fe_1Mn_1Ni_{12}$
$Co_1Cu_1Fe_1Ga_5Ni_{12}$	$Co_1Cu_5Fe_5Sn_1Ni_8$	$Co_1Fe_5Mn_5Pd_1Ni_8$	$Co_1Mn_1Mo_1Pd_{13}Ni_4$	$Co_5Cr_1Fe_5Ga_5Ni_4$
$Co_1Cu_1Fe_5In_1Ni_{12}$	$Co_1Cu_5Ga_1Mn_5Ni_8$	$Co_1Fe_9Mn_1Pd_1Ni_8$	$Co_1Mn_1Mo_1Pd_1Ni_{16}$	$Co_5Cr_1Ga_1Sn_1Ni_{12}$
$Co_1Cu_1Fe_5Pd_5Ni_8$	$Co_1Cu_5Ga_1Pd_1Ni_{12}$	$Co_1Fe_9Mn_1Sn_1Ni_8$	$Co_1Mn_1Mo_1Pd_5Ni_{12}$	$Co_5Cr_1Pd_5Sn_5Ni_4$
$Co_1Cu_1Fe_9Zn_5Ni_4$	$Co_1Cu_5In_1Pd_5Ni_8$	$Co_1Fe_9Mo_1Pd_5Ni_4$	$Co_1Mn_5Mo_1Pd_1Ni_{12}$	$Co_5Cr_1Pd_9Zn_1Ni_4$
$Co_1Cu_1Mn_1Pd_1Ni_{16}$	$Co_1Cu_5Mn_5Pd_1Ni_8$	$Co_1Fe_9Pd_1Sn_1Ni_8$	$Co_1Pd_5Sn_1Zn_5Ni_8$	$Co_5Cr_5Cu_1Mn_5Ni_4$
$Co_1Cu_1Mn_1Zn_1Ni_{16}$	$Co_1Cu_9Mn_1Sn_1Ni_8$	$Co_1Ga_1Mn_1Zn_9Ni_8$	$Co_5Cr_1Cu_1Fe_1Ni_{12}$	$Co_5Cr_5Cu_5Sn_1Ni_4$
$Co_1Cu_1Pd_1Sn_5Ni_{12}$	$Co_1Fe_{13}Ga_1Mo_1Ni_4$	$Co_1Ga_1Mo_5Pd_1Ni_{12}$	$Co_5Cr_1Cu_1Sn_1Ni_{12}$	$Co_5Cr_5Pd_5Sn_1Ni_4$
$Co_1Cu_1Pd_5Zn_1Ni_{12}$	$Co_1Fe_1Ga_1Mn_1Ni_{16}$	$Co_5Fe_1Sn_1Zn_5Ni_8$	$Co_5Cr_1Cu_5Fe_5Ni_4$	$Co_5Cr_5Pd_5Zn_1Ni_4$
$Co_5Cr_9Fe_1Ga_1Ni_4$	$Co_1Fe_1Ga_1Pd_9Ni_8$	$Co_5Fe_5Ga_1Mn_1Ni_8$	$Co_5Ga_1Mo_5Pd_5Ni_4$	$Co_5Mo_1Sn_1Zn_1Ni_{12}$

$Co_5Cr_9Pd_1Zn_1Ni_4$	$Co_5Cu_5Mo_5Pd_1Ni_4$	$Co_5Fe_5Ga_5Mn_1Ni_4$	$Co_5Ga_1Pd_1Sn_5Ni_8$	$Co_5Mo_5Pd_1Sn_1Ni_8$
$Co_5Cu_1Fe_1Sn_1Ni_{12}$	$Co_5Cu_9Ga_1Mo_1Ni_4$	$Co_5Fe_5In_1Mo_5Ni_4$	$Co_5Ga_5Mo_1Sn_1Ni_8$	$Co_5Pd_1Sn_1Zn_1Ni_{12}$
$Co_5Cu_1Fe_5In_1Ni_8$	$Co_5Cu_9Pd_1Sn_1Ni_4$	$Co_5Fe_5Mn_1Pd_5Ni_4$	$Co_5Ga_5Pd_1Zn_1Ni_8$	$Co_9Cr_1Cu_1Pd_1Ni_8$
$Co_5Cu_1Mo_5Pd_1Ni_8$	$Co_5Fe_1In_1Mo_5Ni_8$	$Co_5Fe_5Mo_1Pd_1Ni_8$	$Co_5In_5Mn_1Pd_1Ni_8$	$Co_9Cr_1Fe_1Zn_5Ni_4$
$Co_5Cu_1Mo_5Zn_1Ni_8$	$Co_5Fe_1In_1Zn_1Ni_{12}$	$Co_5Fe_5Pd_5Zn_1Ni_4$	$Co_5Mn_1Pd_1Sn_5Ni_8$	$Co_9Cr_1Fe_5Pd_1Ni_4$
$Co_5Cu_5Ga_1Pd_5Ni_4$	$Co_5Fe_1In_1Zn_5Ni_8$	$Co_5Fe_5Sn_1Zn_5Ni_4$	$Co_5Mn_5Mo_1Pd_1Ni_8$	$Co_9Cr_1Fe_5Zn_1Ni_4$
$Co_5Cu_5Ga_5Mo_1Ni_4$	$Co_5Fe_1Mn_1Mo_1Ni_{12}$	$Co_5Ga_1Mn_5Sn_1Ni_8$	$Co_5Mn_9Pd_1Zn_1Ni_4$	$Co_9Cr_1Mn_1Mo_5Ni_4$
$Co_5Cu_5Ga_5Zn_1Ni_4$	$Co_5Fe_1Mn_5Zn_1Ni_8$	$Co_5Ga_1Mo_1Pd_9Ni_4$	$Co_5Mo_1Pd_1Sn_1Ni_{12}$	$Co_9Cr_1Mo_5Pd_1Ni_4$
$Co_5Cu_5Mn_1Pd_1Ni_8$	$Co_5Fe_1Mo_5Sn_1Ni_8$	$Cr_1Cu_1Mn_1Mo_1Ni_{16}$	$Co_5Mo_1Pd_5Zn_1Ni_8$	$Co_9Cr_1Pd_1Sn_1Ni_8$
$Co_9Cr_5Cu_1Ga_1Ni_4$	$Co_5Fe_1Mo_5Zn_5Ni_4$	$Cr_1Cu_1Mn_1Pd_5Ni_{12}$	$Cr_1Fe_{13}Mo_1Pd_1Ni_4$	$Cr_1Fe_9Ga_1Zn_5Ni_4$
$Co_9Cu_1Fe_1Ga_5Ni_4$	$Co_9Ga_1Pd_5Sn_1Ni_4$	$Cr_1Cu_1Mn_1Zn_1Ni_{16}$	$Cr_1Fe_1Mn_1Pd_1Ni_{16}$	$Cr_1Fe_9Mo_1Zn_1Ni_8$
$Co_9Cu_1Ga_1Pd_1Ni_8$	$Co_9Ga_5Pd_1Sn_1Ni_4$	$Cr_1Cu_1Mo_1Pd_5Ni_{12}$	$Cr_1Fe_1Mo_1Pd_{13}Ni_4$	$Cr_1Fe_9Mo_5Zn_1Ni_4$
$Co_9Cu_1Mn_5Sn_1Ni_4$	$Co_9Pd_1Sn_1Zn_5Ni_4$	$Cr_1Cu_1Pd_5Sn_5Ni_8$	$Cr_1Fe_1Mo_5Zn_5Ni_8$	$Cr_1In_1Mo_1Pd_5Ni_{12}$
$Co_9Fe_1Mn_5Pd_1Ni_4$	$Cr_1Cu_{13}Fe_1Zn_1Ni_4$	$Cr_1Cu_5Fe_1Mn_1Ni_{12}$	$Cr_1Fe_1Pd_{13}Zn_1Ni_4$	$Cr_1Mn_1Mo_5Pd_9Ni_4$
$Co_9Fe_1Mo_1Pd_1Ni_8$	$Cr_1Cu_1Fe_5Ga_5Ni_8$	$Cr_1Cu_5Fe_5Sn_1Ni_8$	$Cr_1Fe_1Sn_1Zn_5Ni_{12}$	$Cr_1Mn_1Pd_{13}Sn_1Ni_4$
$Co_9Fe_5Ga_1Zn_1Ni_4$	$Cr_1Cu_1Fe_5Sn_1Ni_{12}$	$Cr_1Cu_5Ga_1Mo_5Ni_8$	$Cr_1Fe_5Ga_1Pd_1Ni_{12}$	$Cr_1Mn_5Mo_1Zn_5Ni_8$
$Co_9Fe_5Mo_1Sn_1Ni_4$	$Cr_1Cu_1Fe_5Zn_5Ni_8$	$Cr_1Cu_5Ga_5Pd_1Ni_8$	$Cr_1Fe_5In_1Pd_1Ni_{12}$	$Cr_1Mn_5Pd_1Zn_1Ni_{12}$
$Co_9Ga_1Mn_1Pd_5Ni_4$	$Cr_1Cu_1Fe_9Mn_5Ni_4$	$Cr_1Cu_5In_1Pd_9Ni_4$	$Cr_1Fe_5Mn_1Zn_1Ni_{12}$	$Cr_1Pd_{13}Sn_1Zn_1Ni_4$
$Co_9Ga_1Mo_1Zn_1Ni_8$	$Cr_1Cu_1Ga_1Mo_1Ni_{16}$	$Cr_1Cu_5Mo_1Sn_1Ni_{12}$	$Cr_1Fe_5Mo_1Pd_5Ni_8$	$Cr_1Pd_1Sn_1Zn_1Ni_{16}$
$Cr_5Cu_1Fe_1Pd_5Ni_8$	$Cr_5Fe_5Ga_1Pd_5Ni_4$	$Cu_{13}Fe_1Ga_1Pd_1Ni_4$	$Cu_1Fe_5Ga_5Zn_1Ni_8$	$Cu_1Ga_1Pd_1Zn_5Ni_{12}$
$Cr_5Cu_1Mn_1Pd_1Ni_{12}$	$Cr_5Fe_5Mn_1Mo_1Ni_8$	$Cu_{13}Mn_1Mo_1Zn_1Ni_4$	$Cu_1Fe_5Mn_1Pd_9Ni_4$	$Cu_1Ga_1Pd_5Sn_1Ni_{12}$
$Cr_5Cu_1Mn_1Zn_5Ni_8$	$Cr_5Fe_5Mo_1Sn_1Ni_8$	$Cu_{13}Mn_1Sn_1Zn_1Ni_4$	$Cu_1Fe_5Mo_1Pd_5Ni_8$	$Cu_1In_1Mo_1Pd_{13}Ni_4$
$Cr_5Cu_1Sn_1Zn_1Ni_{12}$	$Cr_5Fe_5Pd_1Zn_5Ni_4$	$Cu_1Fe_1Ga_1Mo_1Ni_{16}$	$Cu_1Fe_5Pd_5Sn_1Ni_8$	$Cu_1Mn_1Mo_1Pd_{13}Ni_4$
$Cr_5Cu_5Fe_1Sn_1Ni_8$	$Cr_5Fe_5Pd_5Zn_1Ni_4$	$Cu_1Fe_1Mn_1Mo_1Ni_{16}$	$Cu_1Fe_9Mo_1Zn_5Ni_4$	$Cu_1Mn_1Pd_{13}Zn_1Ni_4$
$Cr_5Cu_5Ga_1Pd_1Ni_8$	$Cr_5Mn_1Mo_1Pd_1Ni_{12}$	$Cu_1Fe_1Mn_5Mo_1Ni_{12}$	$Cu_1Fe_9Pd_1Zn_5Ni_4$	$Cu_1Mn_1Sn_1Zn_5Ni_{12}$
$Cr_5Cu_5Pd_1Zn_1Ni_8$	$Cr_5Mn_1Sn_1Zn_1Ni_{12}$	$Cu_1Fe_1Mn_5Pd_1Ni_{12}$	$Cu_1Ga_1Mn_1Pd_9Ni_8$	$Cu_1Mn_5Mo_1Pd_1Ni_{12}$
$Cr_5Fe_1Ga_1Pd_1Ni_{12}$	$Cr_9Cu_1Fe_1Mn_1Ni_8$	$Cu_1Fe_1Mn_5Pd_5Ni_8$	$Cu_1Ga_1Mn_1Sn_1Ni_{16}$	$Cu_1Mo_1Pd_5Sn_1Ni_{12}$
$Cr_5Fe_1Mn_1Pd_5Ni_8$	$Cr_9Cu_1Fe_1Pd_1Ni_8$	$Cu_1Fe_1Mo_5Zn_1Ni_{12}$	$Cu_1Ga_1Mo_5Pd_5Ni_8$	$Cu_1Mo_5Pd_1Sn_1Ni_{12}$
$Cr_5Fe_1Mo_1Pd_1Ni_{12}$	$Cr_9Fe_1Mn_1Zn_1Ni_8$	$Cu_1Fe_1Pd_1Zn_5Ni_{12}$	$Cu_1Ga_1Mo_5Zn_1Ni_{12}$	$Cu_1Mo_5Pd_5Sn_5Ni_4$
$Cu_1Mo_5Pd_9Sn_1Ni_4$	$Cu_5Ga_1Mo_1Pd_9Ni_4$	$Cu_9Ga_1Mo_1Pd_1Ni_8$	$Fe_1Pd_5Sn_5Zn_1Ni_8$	$Fe_5Mn_5Mo_1Zn_5Ni_4$
$Cu_1Mo_5Pd_9Zn_1Ni_4$	$Cu_5Ga_1Pd_5Sn_5Ni_4$	$Cu_9Ga_1Mo_1Zn_1Ni_8$	$Fe_1Pd_9Sn_1Zn_1Ni_8$	$Fe_5Mo_1Pd_1Sn_1Ni_{12}$
$Cu_1Pd_{13}Sn_1Zn_1Ni_4$	$Cu_5In_1Mn_1Pd_5Ni_8$	$Cu_9Ga_1Pd_5Zn_1Ni_4$	$Fe_5Ga_1Mn_1Pd_1Ni_{12}$	$Fe_5Mo_1Pd_1Zn_5Ni_8$
$Cu_5Fe_1Ga_1Mo_1Ni_{12}$	$Cu_5In_1Mo_5Pd_1Ni_8$	$Fe_{13}Pd_1Sn_1Zn_1Ni_4$	$Fe_5Ga_1Mo_5Sn_1Ni_8$	$Fe_5Mo_1Sn_1Zn_1Ni_{12}$
$Cu_5Fe_1Ga_1Pd_1Ni_{12}$	$Cu_5Mn_1Pd_9Sn_1Ni_4$	$Fe_1Ga_1Mo_5Pd_1Ni_{12}$	$Fe_5Ga_1Pd_9Sn_1Ni_4$	$Fe_5Mo_5Pd_1Zn_1Ni_8$
$Cu_5Fe_1Ga_1Pd_5Ni_8$	$Cu_5Mo_1Sn_1Zn_5Ni_8$	$Fe_1In_1Mo_5Pd_5Ni_8$	$Fe_5In_1Pd_5Sn_1Ni_8$	$Fe_5Mo_5Sn_1Zn_5Ni_4$
$Cu_5Fe_1In_1Zn_9Ni_4$	$Cu_5Mo_5Pd_1Zn_5Ni_4$	$Fe_1Mn_9Pd_1Zn_5Ni_4$	$Fe_5In_1Pd_9Sn_1Ni_4$	$Fe_9Ga_1Mn_1Sn_1Ni_8$
$Cu_5Fe_1Pd_5Sn_1Ni_8$	$Cu_5Pd_1Sn_1Zn_5Ni_8$	$Fe_1Mo_1Pd_{13}Zn_1Ni_4$	$Fe_5Mn_1Mo_1Pd_5Ni_8$	$Fe_9Ga_1Mn_1Zn_1Ni_8$
$Cu_5Fe_5In_1Pd_1Ni_8$	$Cu_9Fe_1Ga_1Sn_1Ni_8$	$Fe_1Mo_1Sn_1Zn_5Ni_{12}$	$Fe_5Mn_1Pd_1Sn_5Ni_8$	$Ga_1Mn_1Sn_1Zn_5Ni_{12}$
$Cu_5Fe_9Mn_1Pd_1Ni_4$	$Cu_9Fe_1Mo_1Pd_5Ni_4$	$Fe_1Mo_5Pd_5Sn_1Ni_8$	$Fe_5Mn_1Pd_9Sn_1Ni_4$	$Ga_1Mo_1Pd_5Sn_5Ni_8$
$Ga_1Mo_1Sn_1Zn_1Ni_{16}$	$Ga_1Mo_5Pd_9Sn_1Ni_4$	$In_1Mo_5Pd_9Zn_1Ni_4$	$Mn_1Mo_1Pd_5Zn_1Ni_{12}$	$Mn_1Pd_{13}Sn_1Zn_1Ni_4$
$Ga_1Mo_5Pd_1Zn_1Ni_{12}$	$In_1Mn_1Mo_1Pd_9Ni_8$	$Mn_1Mo_1Pd_5Sn_5Ni_8$	$Mn_1Mo_5Pd_9Sn_1Ni_4$	$Mo_5Pd_1Sn_5Zn_1Ni_8$

TableS2. The hydrogen adsorption free energies (ΔG_H, eV) for surface sites on $Co_1Pd_5Au_5In_1Ni_8$ and $Co_1Pd_5Au_9In_1Ni_4$ surfaces.

Sites	$Co_1Pd_5Au_5In_1Ni_8$	$Co_1Pd_5Au_9In_1Ni_4$
$Site_1$	-0.30	0.47
$Site_2$	-0.37	0.31
$Site_3$	-0.39	0.37
$Site_4$	-0.37	0.42
$Site_5$	-0.31	0.18
$Site_6$	-0.45	0.70
$Site_7$	-0.37	0.32
$Site_8$	-0.30	0.89
$Site_9$	-0.32	0.31
$Site_{10}$	-0.32	0.63
$Site_{11}$	-0.36	0.52
$Site_{12}$	-0.20	0.47
$Site_{13}$	-0.08	1.29
$Site_{14}$	-0.20	0.35
$Site_{15}$	-0.44	0.35
$Site_{16}$	-0.14	0.25
$Site_{17}$	-0.40	0.30
$Site_{18}$	-0.32	0.30
$Site_{19}$	-0.40	0.56
$Site_{20}$	-0.15	0.34
$Site_{21}$	-0.19	0.32
$Site_{22}$	-0.14	0.33
$Site_{23}$	-0.44	0.37
$Site_{24}$	-0.08	0.34
$Site_{25}$	-0.32	0.37
$Site_{26}$	-0.32	0.94
$Site_{27}$	-0.15	0.53
$Site_{28}$	-0.32	0.61
$Site_{29}$	-0.33	0.29
$Site_{30}$	-0.33	0.66
$Site_{31}$	-0.38	0.29
$Site_{32}$	-0.34	0.33

TableS3. Part list of elemental distributions in the first nearest-neighbor (FNN) regions of surface sites exhibiting near-thermoneutral hydrogen adsorption ($|\Delta G_H| \leq 0.10$ eV).

HEA surface	Site	FNN1	FNN2	FNN3
$Co_1Cr_1Cd_1In_1Ni_{16}$	$Site_{25}$	Ni	Ni	Ni
	$Site_{18}$	Ni	Ni	Co
	$Site_{11}$	Ni	Ni	Co
	$Site_{14}$	Ni	Ni	Cr
	$Site_{7}$	Ni	Ni	Ni
	$Site_{23}$	Ni	Ni	Ni
	$Site_{31}$	Ni	Ni	Ni
	$Site_{20}$	Ni	Co	Cr
$Co_1Cr_1Zn_1Au_1Ni_{16}$	$Site_{11}$	Ni	Co	Zn
	$Site_{21}$	Ni	Ni	Ni
	$Site_{23}$	Ni	Co	Zn
	$Site_{1}$	Ni	Ni	Ni
	$Site_{3}$	Ni	Ni	Cr
	$Site_{14}$	Ni	Zn	Cr
	$Site_{19}$	Ni	Ni	Zn
	$Site_{10}$	Ni	Ni	Co
	$Site_{22}$	Ni	Ni	Ni
	$Site_{31}$	Ni	Ni	Ni
	$Site_{15}$	Ni	Ni	Zn
	$Site_{17}$	Ni	Ni	Ni
	$Site_{13}$	Ni	Zn	Cr
	$Site_{18}$	Ni	Ni	Ni
	$Site_{26}$	Ni	Ni	Ni
	$Site_{24}$	Ni	Ni	Co
	$Site_{7}$	Ni	Ni	Ni
	$Site_{27}$	Ni	Ni	Zn
	$Site_{29}$	Ni	Ni	Zn
	$Site_{12}$	Ni	Ni	Ni
	$Site_{6}$	Ni	Ni	Zn
	$Site_{9}$	Ni	Zn	Cr
	$Site_{30}$	Ni	Ni	Zn
	$Site_{28}$	Ni	Zn	Cr
$Co_1Pd_1Cr_9Zn_5Ni_4$	$Site_{3}$	Co	Cr	Cr
	$Site_{21}$	Zn	Zn	Cr
	$Site_{28}$	Ni	Co	Zn
	$Site_{1}$	Co	Zn	Cr
	$Site_{6}$	Zn	Zn	Cr
	$Site_{23}$	Co	Co	Zn
	$Site_{29}$	Ni	Co	Zn
	$Site_{25}$	Ni	Zn	Cr

	$Site_0$	Co	Co	Zn
	$Site_9$	Ni	Co	Zn
	$Site_5$	Cr	Cr	Cr
	$Site_{22}$	Co	Zn	Cr
	$Site_{14}$	Zn	Cr	Cr
	$Site_{16}$	Ni	Cr	Cr
	$Site_{18}$	Ni	Co	Zn
	$Site_{15}$	Cr	Cr	Cr
	$Site_{10}$	Co	Cr	Cr
	$Site_{12}$	Co	Zn	Cr
	$Site_{19}$	Ni	Ni	Co
	$Site_8$	Ni	Zn	Cr
	$Site_{31}$	Ni	Ni	Zn
	$Site_4$	Co	Zn	Cr
$Co_1Pd_1Ga_1Au_5Ni_{12}$	$Site_{19}$	Ni	Ni	Ni
	$Site_{29}$	Ni	Ni	Ni
	$Site_{14}$	Ni	Ni	Ni
	$Site_{18}$	Ni	Ni	Ni
	$Site_{25}$	Ni	Ni	Ni
	$Site_{21}$	Ni	Ni	Co
	$Site_{22}$	Ni	Ni	Ni
$Co_1Pd_9Cr_1Au_1Ni_8$	$Site_{17}$	Ni	Ni	Ni
	$Site_{27}$	Ni	Ni	Ni
	$Site_{24}$	Ni	Ni	Ni
	$Site_3$	Ni	Ni	Ni
	$Site_{21}$	Ni	Ni	Ni
	$Site_{10}$	Ni	Ni	Ni
	$Site_{25}$	Ni	Ni	Ni
	$Site_5$	Ni	Ni	Ni
	$Site_9$	Ni	Ni	Ni
	$Site_{28}$	Ni	Ni	Ni
	$Site_7$	Ni	Ni	Ni
	$Site_{19}$	Ni	Ni	Co
$Co_1Pd_1Zn_5Ga_1Ni_{12}$	$Site_0$	Ni	Ni	Zn
	$Site_7$	Ni	Ni	Zn
	$Site_{24}$	Ni	Ni	Ni
	$Site_2$	Ni	Ni	Zn
	$Site_{10}$	Ni	Ni	Ni
	$Site_{19}$	Ni	Ni	Zn
	$Site_{27}$	Ni	Co	Zn
	$Site_{20}$	Ni	Ni	Zn
	$Site_{29}$	Ni	Ni	Zn
	$Site_1$	Ni	Ni	Zn

$Co_1Pd_1Zn_5Ga_1Ni_{12}$	$Site_{11}$	Ni	Ni	Zn
	$Site_{18}$	Ni	Ni	Co
	$Site_4$	Ni	Co	Zn
	$Site_{21}$	Ni	Co	Zn
	$Site_{28}$	Ni	Co	Zn
$Co_1Pd_9Cr_1Ag_1Ni_8$	$Site_{19}$	Ni	Ni	Ni
	$Site_{12}$	Ni	Ni	Co
	$Site_{25}$	Ni	Ni	Ni
	$Site_{30}$	Ni	Ni	Cr
	$Site_{28}$	Ni	Ni	Ni
	$Site_{27}$	Ni	Ni	Cr
$Co_1Pd_5Cr_1In_1Ni_{12}$	$Site_{13}$	Ni	Ni	Ni
	$Site_{18}$	Ni	Ni	Ni
	$Site_{27}$	Ni	Ni	Ni
	$Site_{30}$	Ni	Ni	Cr
	$Site_{31}$	Ni	Ni	Cr
	$Site_{22}$	Ni	Ni	Ni
	$Site_{17}$	Ni	Ni	Ni
	$Site_{26}$	Ni	Ni	Ni
	$Site_{29}$	Ni	Ni	Cr
$Co_1Pd_5Ga_1Ag_1Ni_{12}$	$Site_6$	Ni	Ni	Co
	$Site_{24}$	Ni	Ni	Ni
	$Site_{15}$	Ni	Ni	Ni
	$Site_{13}$	Ni	Ni	Ni
	$Site_{16}$	Ni	Ni	Co
$Co_1Pd_5Ga_1Cd_1Ni_{12}$	$Site_{31}$	Ni	Ni	Ni
	$Site_{21}$	Ni	Ni	Ni
	$Site_4$	Ni	Ni	Co
	$Site_6$	Ni	Ni	Ni
	$Site_{28}$	Ni	Ni	Ni
$Co_1Pd_5Zn_1Au_9Ni_4$	$Site_{10}$	Ni	Ni	Co
$Co_1Sn_1Pd_9Ag_1Ni_8$	$Site_4$	Ag	Pd	Ni
	$Site_9$	Ag	Ni	Pd
	$Site_2$	Ag	Ni	Pd
$Co_1Sn_1Pd_1Cr_1Ni_{16}$	$Site_{13}$	Ni	Ni	Ni
	$Site_4$	Ni	Ni	Ni
	$Site_{12}$	Ni	Ni	Ni
	$Site_{30}$	Ni	Ni	Cr
	$Site_{21}$	Ni	Ni	Ni
	$Site_{28}$	Ni	Ni	Co
	$Site_{10}$	Ni	Ni	Co
	$Site_{27}$	Ni	Co	Cr

TableS4. Part list of proposed high-entropy alloy (HEA) catalysts.

Quaternary high-entropy alloys	Quinary high-entropy alloys
$Sn_1Zn_1Ga_1Ni_{17}$	$Mn_1Mo_1Co_1Ga_1Ni_{16}$
$Cu_1Co_9Cr_1Ni_9$	$Co_5Sn_1Cr_1Zn_1Ni_{12}$
$Fe_1Co_1Zn_1Ni_{17}$	$Mo_1Co_5Cr_1Ga_1Ni_{12}$
$Cu_1Fe_1Ga_1Ni_{17}$	$Co_5Cr_1Zn_1Ga_1Ni_{12}$
$Cu_1Fe_1Cr_5Ni_{13}$	$Mo_1Sn_1Zn_1Ga_1Ni_{16}$
$Co_5Ga_1Cd_1Ni_{13}$	$Cu_1Co_1Sn_1Cr_1Ni_{16}$
$Mn_1Cu_1Sn_1Ni_{17}$	$Cu_1Co_5Ga_1Cd_1Ni_{12}$

Table S5. Comparison of hydrogen adsorption free energies (ΔG_H, eV) for various surface sites of S1 (Fig. S4) with and without van der Waals (vdw) corrections.

Sites	ΔG_H (without vdw correction)	ΔG_H (with vdw correction)
H1	-0.41	-0.46
T1	-0.53	-0.58
B1	-0.43	-0.46
H2	-0.41	-0.44
T2	-0.54	-0.58
B2	-0.48	-0.53
H3	-0.44	-0.46
T3	-0.40	-0.42
B3	-0.45	-0.47

References

1. G. Kresse and J. Furthmüller, Phys. Rev. B, 1996, 54, 11169–11186.
2. G. Kresse and J. Furthmüller, Comput. Mater. Sci., 1996, 6, 15–50.
3. A. Hjorth Larsen, J. Jorgen Mortensen, J. Blomqvist, I. E. Castelli, R. Christensen, M. Dulak, J. Friis, M. N. Groves, B. Hammer, C. Hargus, E. D. Hermes, P. C. Jennings, P. Bjerre Jensen, J. Kermode, J. R. Kitchin, E. Leonhard Kolsbjerg, J. Kubal, K. Kaasbjerg, S. Lysgaard, J. Bergmann Maronsson, T. Maxson, T. Olsen, L. Pastewka, A. Peterson, C. Rostgaard, J. Schiotz, O. Schutt, M. Strange, K. S. Thygesen, T. Vegge, L. Vilhelmsen, M. Walter, Z. Zeng and K. W. Jacobsen, J. Phys.: Condens. Matter, 2017, 29, 273002.
4. P. E. Blochl, Phys. Rev. B, 1994, 50, 17953–17979.
5. J. P. Perdew, K. Burke and M. Ernzerhof, Phys. Rev. Lett., 1996, 77, 3865–3868.
6. C. Adamo and V. Barone, J. Chem. Phys., 1999, 110, 6158–6170.
7. M. Ernzerhof and G. E. Scuseria, J. Chem. Phys., 1999, 110, 5029–5036.
8. J. D. Pack and H. J. Monkhorst, Phys. Rev. B, 1977, 16, 1748–1749.
9. Y. Zhu, S. Jiang, B. Feng, Y. Wang, M. Fang, H. Sun and W. Liu, Chin. Chem. Lett. [Preprint], 2026, Available from: https://doi.org/10.1016/j.cclet.2026.112720.
10. J. K. R. Nørskov, J.; Logadottir, A.; Lindqvist, L.; Kitchin, J. R.; Bligaard, T.; Jónsson, H., J. Phys. Chem. B, 2004, 108, 17886−17892.
11. V. Wang, N. Xu, J.-C. Liu, G. Tang and W.-T. Geng, Comput. Phys. Commun., 2021, 267, 108033.
12. D. H. Mok and S. Back, J. Chem. Inf. Model., 2021, 61, 4514–4520.
13. G. Cao, S. Yang, J. C. Ren and W. Liu, Nat. Commun., 2025, 16, 1251.
14. Z. W. Chen, J. Li, P. Ou, J. E. Huang, Z. Wen, L. Chen, X. Yao, G. Cai, C. C. Yang, C. V. Singh and Q. Jiang, Nat Commun, 2024, 15, 359.